Journal of Power Sources 225 (2013) 34–39

Contents lists available at SciVerse ScienceDirect

Journal of Power Sources

journal homepage: www.elsevier.com/locate/jpowsour

Short communication

Solid-state synthesis of $LiCoO_2/LiCo_{0.99}Ti_{0.01}O_2$ composite as cathode material for lithium ion batteries

Jinpeng Yu [a,b], Zenghui Han [a], Xiaohong Hu [a], Hui Zhan [a,*], Yunhong Zhou [a], Xingjiang Liu [b]

[a] College of Chemistry and Molecular Sciences, Wuhan University, Wuhan 430072, China
[b] National Key Laboratory of Power Source, Tianjin Institute of Power Sources, Tianjin 300381, China

HIGHLIGHTS

- We have fabricated a micron-sized $LiCoO_2/LiCo_{0.99}Ti_{0.01}O_2$ composite by solid-phase synthesis.
- XPS measurement and SEM observation reveal a Ti concentration gradient in the composite.
- The obtained $LiCoO_2/LiCo_{0.99}Ti_{0.01}O_2$ composite presents greatly enhanced cycling stability as well as rate capability.
- DSC further indicates that the $LiCoO_2/LiCo_{0.99}Ti_{0.01}O_2$ composite has a better thermal stability than the bare $LiCoO_2$.

ARTICLE INFO

Article history:
Received 10 June 2012
Received in revised form
27 August 2012
Accepted 14 September 2012
Available online 11 October 2012

Keywords:
Core-shell structure
Layered compound
Lithium batteries
Solid-phase synthesis

ABSTRACT

We have fabricated a micron-sized $LiCoO_2/LiCo_{0.99}Ti_{0.01}O_2$ composite successfully by solid-phase synthesis, its core-shell structure has been proved by SEM and XPS observation. Electrochemical examinations show that comparing with $LiCoO_2$ and $LiCo_{0.99}Ti_{0.01}O_2$, the obtained $LiCoO_2/LiCo_{0.99}Ti_{0.01}O_2$ composite presents greatly enhanced cycling stability as well as rate capability. In addition, DSC measurement indicates that $LiCoO_2/LiCo_{0.99}Ti_{0.01}O_2$ has a better thermal safety than $LiCoO_2$. It is considered that all the improvement should be explained by the particular core-shell morphology of the $LiCoO_2/LiCo_{0.99}Ti_{0.01}O_2$ sample.

1. Introduction

The fabrication of the core-shell structure particles has attracted considerable attention in recent years because of their potential use for photonic crystals, catalysts, diagnostics, pharmacology, etc [1–3]. In particular, it has been producing important and profound effect on the development of lithium ion batteries for energy storage and EV applications, since this novel strategy is introduced for preparing electrode materials with improved performances [4–9]. It is also believed that the inorganics with high electro-activity is one of the best choices in various "shell" materials [7,10–14]. However, the coating procedures are usually complicated or require the use of expensive reactants, leading to difficulties in mass production. In view of commercial applications, a facile and cost-effective alternate is still required.

$LiCoO_2$ is one of the most important cathode materials at the present time [15]. Nevertheless, its practical capacity of 140 mAh g^{-1} is almost only half of the theoretical value and a further charge up to 4.3 V or higher voltage usually incurs severe capacity loss [16]. To overcome the bad cycleability under high upper-limit voltage charging, doping, as well as surface coating has been widely investigated and substantially proved to be an effective way [17–20]. However, for the doping strategy, the substituted phase of $LiCo_{1-x}M_xO_2$ (M = metal and transition metal ions) usually has lower average particle size than pristine $LiCoO_2$ [17,19,21–23], such as $LiCo_{1-x}Ti_xO_2$, which finally leads to lower volume specific energy density of the cell.

Based on the above cognition and the requirement for mass production, we propose a high-temperature calcination route to obtain $LiCoO_2/LiCo_{0.99}Ti_{0.01}O_2$ composite with $LiCoO_2$ substrate and $LiCo_{0.99}Ti_{0.01}O_2$ surface layer. The preparation of $LiCoO_2/LiCo_{0.99}Ti_{0.01}O_2$ composite is described in Section 2. Briefly, two annealing treatments are involved in the obtaining of $LiCoO_2$ core and then $LiCoO_2/LiCo_{0.99}Ti_{0.01}O_2$ composite. It is expected that the synthesis

* Corresponding author. Tel.: +86 27 68756931; fax: +86 27 68754067.
E-mail address: zhanhui3620@126.com (H. Zhan).

0378-7753/$ – see front matter © 2012 Elsevier B.V. All rights reserved.
http://dx.doi.org/10.1016/j.jpowsour.2012.09.050

route can well deal with the balance between body-doping and surface coating approaches, and thus the materials with the similar particle size as pristine $LiCoO_2$ and improved cycling stability and rate capability can be obtained. Besides, the pristine $LiCoO_2$ and the doping phase of $LiCo_{0.99}Ti_{0.01}O_2$ were also prepared as the reference through a similar solid-state route. Their structural and electrochemical characteristics are investigated in terms of XRD, SEM, XPS and electrochemical measurements.

2. Experimental

The $LiCo_{0.99}Ti_{0.01}O_2$ materials were prepared by high-temperature calcination from the mixture of Li_2CO_3, Co_3O_4 and TiO_2 in air, in which the molar ratio of Li:Co:Ti was 1.05:0.99:0.01. Excess Li_2CO_3 was used to compensate for the loss of Li during firing. The finely ground mixtures were first heated at 850 °C for 10 h and then annealed at 920 °C for another 10 h without intermediate grinding. $LiCoO_2$ was prepared through the same procedure except without TiO_2 adding. The synthesis of the $LiCoO_2$/$LiCo_{0.99}Ti_{0.01}O_2$ composite was as follows: the mixture of Li_2CO_3, Co_3O_4 and TiO_2 (molar ratio = 1.05: 0.99: 0.01) was blend with the as-prepared $LiCoO_2$, and then the mixture was also heated following the above-mentioned procedure. In the final product, the nominal molar ratio of $LiCoO_2$:$LiCo_{0.99}Ti_{0.01}O_2$ is 1:0.2.

XRD analysis was conducted with XRD-6000 diffractometer (Shimadzu, Japan), Cu Kα radiation and a scan rate of 4 °C min^{-1}. The morphology of the samples was observed on a Quanta 200 scanning electron microscope (SEM). The particle size and particle size distribution were determined further by laser scattering measurements (Mastersizer 2000, U. K.). X-ray photoelectron spectroscopy (XPS) data were obtained using an ESCALab250 electron spectrometer from Thermo Scientific Corporation with monochromatic 150 W Al Kα radiation. The base pressure was about 6.5×10^{-10} mbar. The binding energies were referenced to the C1s line at 284.8 eV from alkyl or adventitious carbon. Thermal characterization of the products was done on a Universal V4.3A TA DSC. The measurements were conducted in air from ambient temperature to 400 °C at a heating rate of 20 °C min^{-1}, and all electrodes were charged to 4.7 V for 8 h before being subjected to DSC measurement.

Galvanostatic cycling was performed on 2016 coin cells. The cathode electrode was made by mixing 80 wt. % active material, 10 wt. % PTFE binder and 10 wt. % acetylene black, then pressing them on an aluminium mesh. Thus prepared electrode was dried at 150 °C for 12 h before the cell assembling. Metallic lithium was used as the anode. The electrolyte was 1 M $LiPF_6$ in a 1:1 volume ratio mixture of ethylene carbonate (EC)/dimethyl carbonate (DMC), and the separator was Celgard 2300 membrane. The cells were assembled in the argon filled glove box (MECABOX80-1"s", Switzerland).

3. Results and discussion

The powder XRD patterns of $LiCoO_2$, $LiCo_{0.99}Ti_{0.01}O_2$ and the $LiCoO_2$/$LiCo_{0.99}Ti_{0.01}O_2$ composite are compared in Fig. 1. All the powders have a well-defined hexagonal α-$NaFeO_2$ structure. No impurity phases, such as Co_3O_4 or TiO_2 can be detected. But considering the small amount of Ti in the final product of $LiCoO_2$/$LiCo_{0.99}Ti_{0.01}O_2$ composite or $LiCo_{0.99}Ti_{0.01}O_2$, this is not enough to exclude the existence of Ti-containing impurity at the grain boundary. Cell parameters are determined by Rietveld method, and the results are given in Table 1. Comparing with $LiCoO_2$, the other two phases do not show significant differences except the $LiCo_{0.99}Ti_{0.01}O_2$ sample has a slightly decreased cell volume. Grain size can be estimated from the FWHM value. Based on the Scherrer

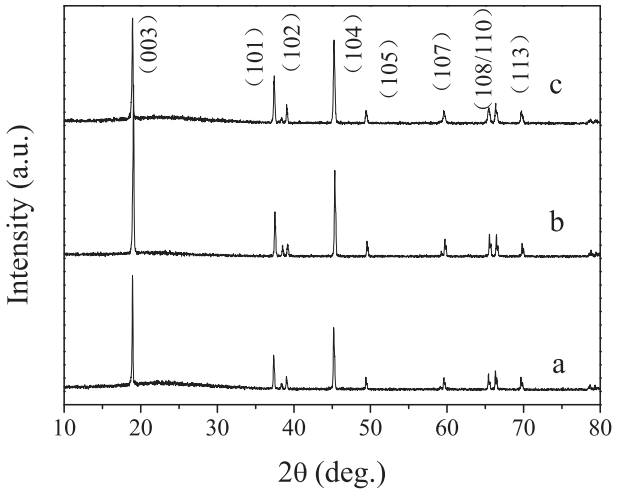

Fig. 1. XRD patterns of (a) $LiCoO_2$, (b) $LiCoO_2$/$LiCo_{0.99}Ti_{0.01}O_2$ composite and (c) $LiCo_{0.99}Ti_{0.01}O_2$.

formula of $D_{hkl} = k\lambda/\beta\cos\theta$, grain size of $LiCoO_2$, $LiCo_{0.99}Ti_{0.01}O_2$ and $LiCoO_2$/$LiCo_{0.99}Ti_{0.01}O_2$ can be determined as 86.28 nm, 62.88 nm and 83.35 nm, respectively (FWHM value of the [104] peak was used in the calculation). Obviously, Ti doping leads to a reduced grain size.

The variation in the particle size or particle morphology can be evidenced by SEM observation. From Fig 2, $LiCoO_2$ and $LiCoO_2$/$LiCo_{0.99}Ti_{0.01}O_2$ shows similar particle morphology and both appear as blocks, and their surface is quite smooth. Additionally, SEM images indicate that, as the particle size is concerned, $LiCo_{0.99}Ti_{0.01}O_2$ is the smallest, while the pristine $LiCoO_2$ is the largest and $LiCoO_2$/$LiCo_{0.99}Ti_{0.01}O_2$ is in between. This observation is in agreement with the result of particle size distribution analysis in Table 2. Among the three studied samples, $LiCoO_2$/$LiCo_{0.99}Ti_{0.01}O_2$ shows the most uniform particle size distribution, and its average particle size is bigger than $LiCo_{0.99}Ti_{0.01}O_2$ but smaller than $LiCoO_2$. The data in Table 2 further implies that the packing density of the resulting samples should vary in the order of $LiCoO_2 > LiCoO_2$/$LiCo_{0.99}Ti_{0.01}O_2 > LiCo_{0.99}Ti_{0.01}O_2$.

SEM measurement reveals the particular morphology of the $LiCoO_2$/$LiCo_{0.99}Ti_{0.01}O_2$ composite. $LiCoO_2$/$LiCo_{0.99}Ti_{0.01}O_2$ composite was ground in an agate mortar and then subjected to SEM observation. Fig. 3a shows the SEM micrograph of the partially crushed particle. From the crack, we can discern two layers, the inner layer should be the $LiCoO_2$ substrate and the outer layer should be the $LiCo_{0.99}Ti_{0.01}O_2$ shell. It is also noticed that the shell layer is not smooth but rather rough. We conjecture that the particular morphology is caused by the encapsulation of $LiCoO_2$ substrate within the Li—Ti—Co oxide phase. Our speculation about the core-shell structure has been further confirmed by XPS measurements. Ar ion etching was used to examine the concentration depth profiles of the $LiCoO_2$/$LiCo_{0.99}Ti_{0.01}O_2$ powder. Fig. 3b shows the Ti2p and Co2p spectrum with different sputtering time. The intensity for Ti becomes lower gradually upon Ar^+ etching. After 810s' etching, it is hardly visible, suggesting a Ti concentration

Table 1
Lattice parameters of $LiCoO_2$, $LiCo_{0.99}Ti_{0.01}O_2$ and $LiCoO_2$/$LiCo_{0.99}Ti_{0.01}O_2$ samples.

Sample	a (Å)	b (Å)	V (Å^3)
$LiCoO_2$	2.8168	14.0553	96.58
$LiCo_{0.99}Ti_{0.01}O_2$	2.8159	14.0575	95.63
$LiCoO_2$/0.2$LiCo_{0.99}Ti_{0.01}O_2$	2.8169	14.0591	96.61

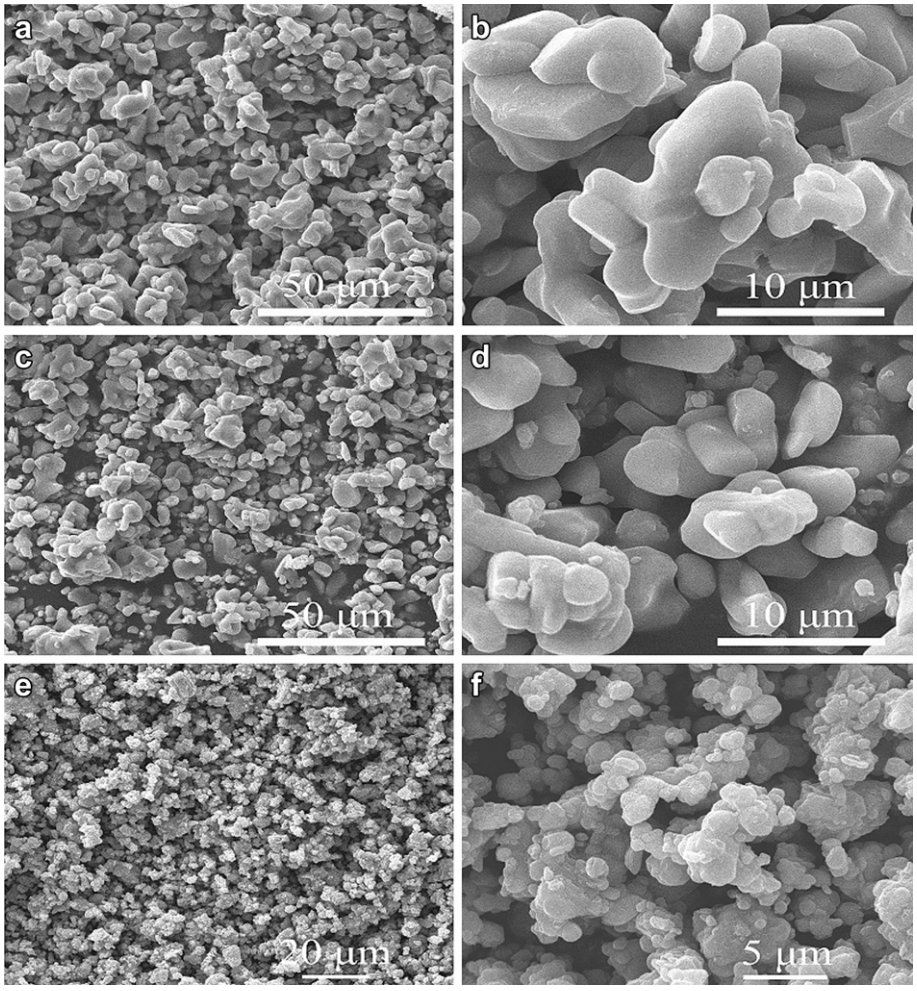

Fig. 2. SEM images of (a and b) $LiCoO_2$; (c and d) $LiCoO_2/LiCo0_{.99}Ti_{0.01}O_2$; and (e and f) $LiCo_{0.99}Ti_{0.01}O_2$.

Table 2
The result of particle size distribution analysis on $LiCoO_2$, $LiCo_{0.99}Ti_{0.01}O_2$ and $LiCoO_2/LiCo_{0.99}Ti_{0.01}O_2$ powders.

Samples	D_{10} (μm)	D_{50} (μm)	D_{90} (μm)
$LiCoO_2$	7.551	16.492	33.756
$LiCo_{0.99}Ti_{0.01}O_2$	5.005	10.596	21.075
$LiCoO_2/0.2LiCo_{0.99}Ti_{0.01}O_2$	7.359	12.958	21.834

gradient may exist in $LiCoO_2/LiCo_{0.99}Ti_{0.01}O_2$ sample and Ti is more likely to be enriched in the surface layer. It could be explained by the Ti diffusion from the shell to the core during high-temperature calcination. On the other hand, the intensity for Co becomes slightly higher with Ar^+ etching, but changes insignificantly after 510s' etching, indicating the relatively stable concentration of Co in the product.

The unique structure is expected to improve the electrochemical performance of the composite. Fig. 4 presents the first charge and

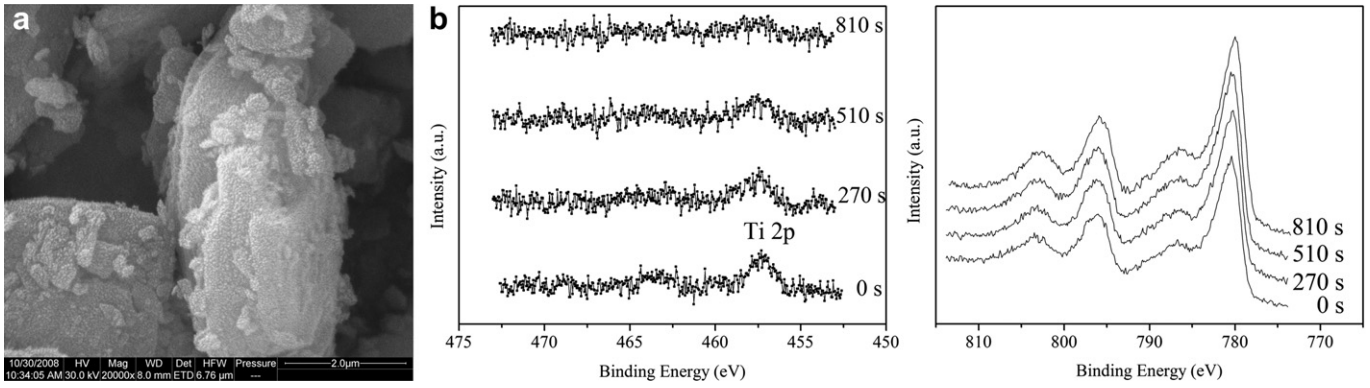

Fig. 3. (a) SEM images of the partially crushed $LiCoO_2/LiCo_{0.99}Ti_{0.01}O_2$ particle; (b) Ti2p and Co2p XPS spectra of $LiCoO_2/LiCo_{0.99}Ti_{0.01}O_2$ material with different sputtering time.

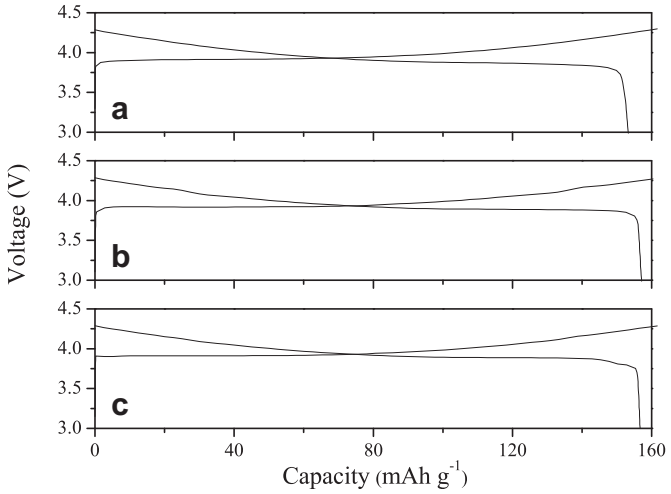

Fig. 4. The initial charge and discharge curves of (a) $LiCoO_2$, (b) $LiCo_{0.99}Ti_{0.01}O_2$ and (c) $LiCoO_2/LiCo_{0.99}Ti_{0.01}O_2$ at room temperature. (Potential range: 3.0–4.3 V, current: 30 mA g^{-1}).

discharge profiles of the resulting samples. It can be seen that the charge and the discharge curves of the three electrodes are not distinctly different from each other in the initial cycle. This is understandable in view of the fact that the charge–discharge mechanisms are same for these materials. Besides, the first discharge capacity of $LiCoO_2$, $LiCo_{0.99}Ti_{0.01}O_2$ and $LiCoO_2/LiCo_{0.99}Ti_{0.01}O_2$ is about 153.3, 157.1 and 156.7 mAh g^{-1}, respectively, corresponding to the efficiency of 94.7%, 95.1% and 95.8% for each sample. Cycling tests were carried out following a given procedure. The cells were cycled at 30 mA g^{-1} in the first two cycles, then cycling was continued at 10 mA g^{-1} between 3.0 and 4.3 V at room temperature. The variation of discharge capacity with cycle number is shown in Fig. 5a for the $LiCoO_2$, $LiCo_{0.99}Ti_{0.01}O_2$ and $LiCoO_2/LiCo_{0.99}Ti_{0.01}O_2$ materials. As been expected, the results indicate that the capacity retention with cycling of the composite is as good as that of the $LiCo_{0.99}Ti_{0.01}O_2$, and significantly superior to pristine $LiCoO_2$ at room temperature in the potential range of 3–4.3 V. The merit of the $LiCoO_2/LiCo_{0.99}Ti_{0.01}O_2$ composite phase is more evidenced in Fig. 5b. When the charge limit is increased to 4.4 V, $LiCoO_2/LiCo_{0.99}Ti_{0.01}O_2$ composite phase still shows the cycling stability as good as that of $LiCo_{0.99}Ti_{0.01}O_2$, as the pristine $LiCoO_2$ has a very poor cycling performance in this potential range (not shown here). The results mean that the $LiCoO_2/LiCo_{0.99}Ti_{0.01}O_2$ composite has an obviously improved cycling stability when

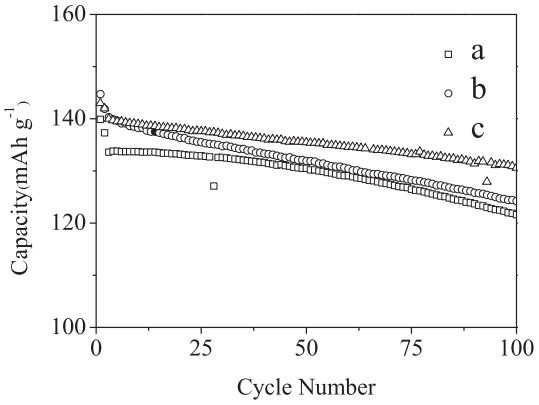

Fig. 6. Cycling performance of (a) $LiCoO_2$, (b) $LiCo_{0.99}Ti_{0.01}O_2$ and (c) $LiCoO_2/LiCo_{0.99}Ti_{0.01}O_2$ between 3.0 and 4.2 V at 60 °C.

a higher charge voltage is applied, combined with its particle size characteristic, it is a good material for practical use.

In Fig. 6, the cycling stability of $LiCoO_2/LiCo_{0.99}Ti_{0.01}O_2$ at 60 °C is shown and compared with that of $LiCoO_2$ and $LiCo_{0.99}Ti_{0.01}O_2$. All the cells were cycled at 30 mA g^{-1} in the first two cycles, then cycling was continued at 100 mA g^{-1} between 3.0 and 4.2 V. Among all the studied electrodes, the $LiCoO_2/LiCo_{0.99}Ti_{0.01}O_2$ composite shows the best cycling property, with the capacity of 130.6 mAh g^{-1} after 100th cycle.

In addition to the cycling stability, $LiCoO_2/LiCo_{0.99}Ti_{0.01}O_2$ composite presents a greatly enhanced rate performance in the voltage range of 3.0–4.2 V. In Fig. 7, the capacity vs. current rate of

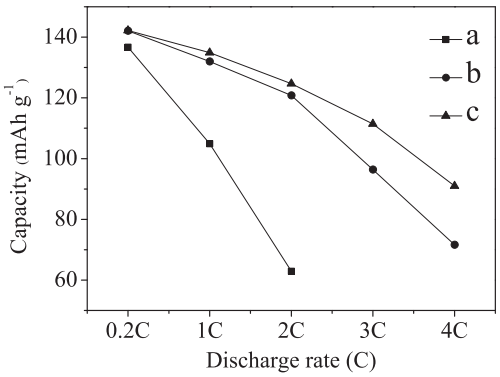

Fig. 7. Comparison of the rate performance of (a) $LiCoO_2$, (b) $LiCo_{0.99}Ti_{0.01}O_2$ and (c) $LiCoO_2/LiCo_{0.99}Ti_{0.01}O_2$ materials. (Potential range: 3.0–4.2 V).

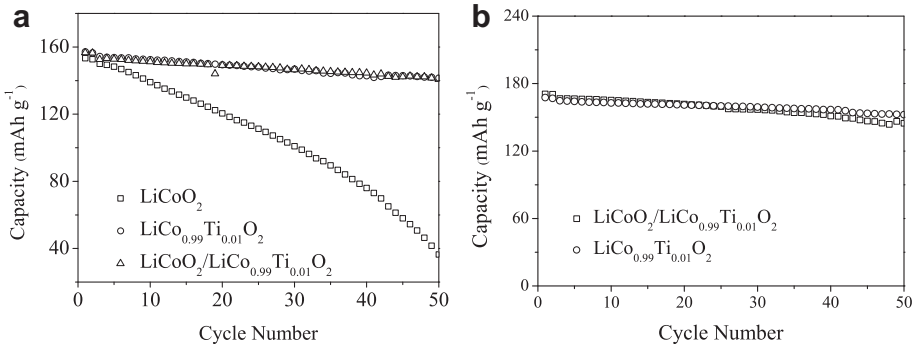

Fig. 5. (a) Comparison of the cycling stability of $LiCoO_2$, $LiCo_{0.99}Ti_{0.01}O_2$ and $LiCoO_2/LiCo_{0.99}Ti_{0.01}O_2$ between 3.0 and 4.3 V at room temperature; (b) the cycling performance of $LiCoO_2/LiCo_{0.99}Ti_{0.01}O_2$ and $LiCo_{0.99}Ti_{0.01}O_2$ between 3.0 and 4.4 V at room temperature.

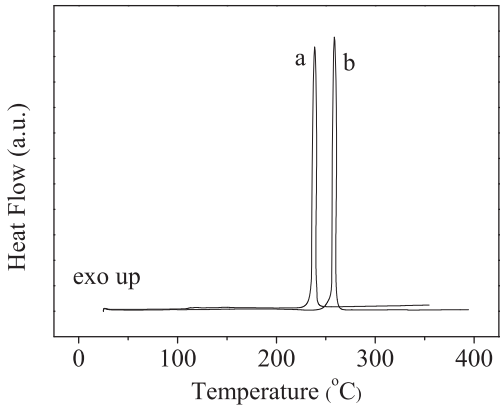

Fig. 8. DSC traces of (a) $LiCoO_2$ and (b) $LiCoO_2/LiCo_{0.99}Ti_{0.01}O_2$.

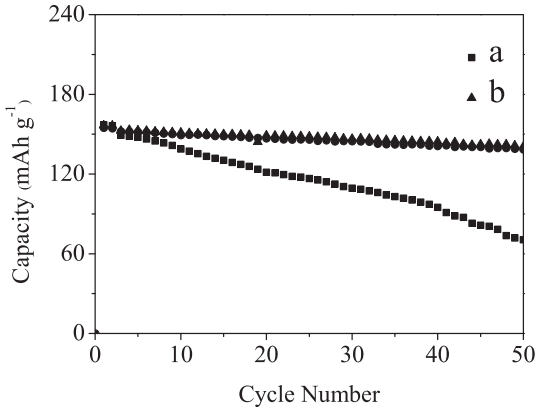

Fig. 10. Comparison of the cycling stability of (a) the grinded mixture of $LiCoO_2$ and $LiCo_{0.99}Ti_{0.01}O_2$ and (b) $LiCoO_2/LiCo_{0.99}Ti_{0.01}O_2$ composite between 3.0 and 4.3 V at room temperature.

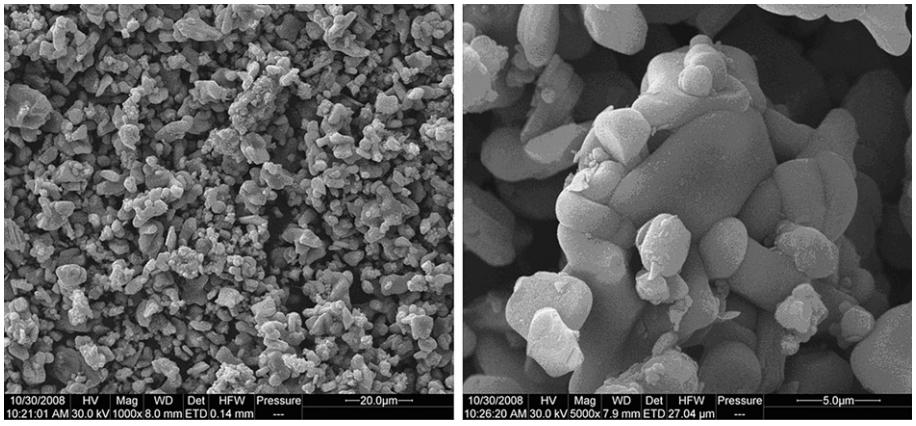

Fig. 9. SEM images of the grinded mixture of $LiCoO_2$ and $LiCo_{0.99}Ti_{0.01}O_2$.

all the resulting samples is compared. For pristine $LiCoO_2$, the discharging capacity at 2C rate is no more than 50% of the capacity at 0.2C (1C = 140 mA g^{-1}). While for $LiCoO_2/LiCo_{0.99}Ti_{0.01}O_2$, $C_{4C}/C_{0.2C}$ (the ratio of capacity under 4C: capacity under 0.2C) is as high as 64%, even much better than the doping phase of $LiCo_{0.99}Ti_{0.01}O_2$, whose $C_{4C}/C_{0.2C}$ is less than 50%. Obviously, the particular core-shell structure of $LiCoO_2/LiCo_{0.99}Ti_{0.01}O_2$ should be accounted for its improved rate performance as well as cycling stability.

Besides the electrochemical property, thermal stability is another important concern for the cathode material of lithium ion battery, especially for the layer-structured $LiCoO_2$, whose thermal safety has been criticized often. Fig. 8 compares the differential scanning calorimetry (DSC) traces of $LiCoO_2$ and the $LiCoO_2/LiCo_{0.99}Ti_{0.01}O_2$ composite electrode charged to 4.7 V. The results show that the exothermic reaction temperature of the composite is delayed to 258.55 °C from 238.63 °C for the bare $LiCoO_2$, although the exothermic amounts are close to each other. Therefore, we think that the thermally stable outer shell of $LiCo_{0.99}Ti_{0.01}O_2$ could suppress the oxygen release from the highly delithiated $Li_{1-x}CoO_2$ and improves the thermal stability of the material at charged state.

It may be argued that a thorough mixing of $LiCoO_2$ and $LiCo_{0.99}Ti_{0.01}O_2$ can achieve a similar electrochemical property presented by the $LiCoO_2/LiCo_{0.99}Ti_{0.01}O_2$ core-shell phase. To better understand the mechanism of the electrochemical property improvement in $LiCoO_2/LiCo_{0.99}Ti_{0.01}O_2$, above-mentioned $LiCoO_2$ and $LiCo_{0.99}Ti_{0.01}O_2$ sample was grinded to obtain their mixture with the molar ratio of $LiCoO_2$:$LiCo_{0.99}Ti_{0.01}O_2$ = 1:0.2. Fig. 9 illustrates its SEM image. We can see that comparing with the SEM photos of $LiCoO_2/LiCo_{0.99}Ti_{0.01}O_2$ composite, the mixture shows the combination of the morphology characteristic of $LiCoO_2$ and $LiCo_{0.99}Ti_{0.01}O_2$. The larger particle represents the $LiCoO_2$ phase, while the much smaller crumbs adhering to the large particle represents $LiCo_{0.99}Ti_{0.01}O_2$. Further comparison of the cycling behaviour of the mixture and $LiCoO_2/LiCo_{0.99}Ti_{0.01}O_2$ phase can reveal more differences. Fig. 10 displays the capacity vs. cycle number plots of these two samples. The test condition is consistent with that in Fig. 5a. The results prove the much better cycling stability of the $LiCoO_2/LiCo_{0.99}Ti_{0.01}O_2$ phase than the mixture of $LiCoO_2$ and $LiCo_{0.99}Ti_{0.01}O_2$. Obviously, it should be explained by the particular core-shell structure of the former phase, and it may further imply that although $LiCoO_2/LiCo_{0.99}Ti_{0.01}O_2$ phase and the mixture of $LiCoO_2$ and $LiCo_{0.99}Ti_{0.01}O_2$ both contains Ti, building a Ti concentration gradient in the product is more beneficial for the electrochemical performance.

4. Conclusion

We have fabricated a micron-sized $LiCoO_2/LiCo_{0.99}Ti_{0.01}O_2$ composite with the core-shell structure successfully by solid-phase synthesis. As compared with $LiCoO_2$, the obtained phase shows a greatly improved cycling stability and rate capability while maintaining a similar particle size as $LiCoO_2$. XPS measurement and SEM observation reveal a Ti concentration gradient in

$LiCoO_2/LiCo_{0.99}Ti_{0.01}O_2$ composite and its core-shell particle characteristic. DSC further indicates that the $LiCoO_2/LiCo_{0.99}Ti_{0.01}O_2$ composite has a better thermal stability than the bare $LiCoO_2$. Because of the facile preparation, greatly enhanced electrochemical property and thermal stability, $LiCoO_2/LiCo_{0.99}Ti_{0.01}O_2$ composite is believed to be a good cathode material for practical use.

Acknowledgements

Authors would express their sincere thanks to the Nature Science Foundation of China (No. 20873094, 21073138) for the financial support.

References

[1] S. Alayoglu, A.U. Nilekar, M. Mavrikakis, B. Eichorn, Nat. Mater. 7 (2008) 333–338.
[2] Y. Wang, S. Gao, W.-H. Ye, H.S. Yoon, Y.-Y. Yang, Nat. Mater. 5 (2006) 791–796.
[3] G. Schneider, G. Decher, N. Nerambourg, R. Praho, M.H.V. Werts, M. Blanchard-Desce, Nano Lett. 6 (2006) 530–536.
[4] J. Cho, Y.J. Kim, B. Park, Chem. Mater. 12 (2000) 3788–3791.
[5] J. Cho, Y.J. Kim, B. Park, Angew. Chem. Int. Ed. 113 (2001) 3471–3473, Angew. Chem. Int. Ed. 40 (2001) 3367–3369.
[6] J. Cho, Y.W. Kim, B. Kim, J.G. Lee, B. Park, Angew. Chem. Int. Ed. 115 (2003) 1656–1659, Angew. Chem. Int. Ed. 42 (2003) 1618–1621.
[7] Y.-K. Sun, S.-T. Myung, M.-H. Kim, J. Prakash, K. Amine, J. Am. Chem. Soc. 127 (2005) 13411–13418.
[8] K.T. Lee, Y.S. Jung, S.M. Oh, J. Am. Chem. Soc. 125 (2003) 5652–5653.
[9] Y. Wang, Y. Wang, E. Hosono, K. Wang, H. Zhou, Angew. Chem. Int. Ed. 120 (2008) 7571–7575, Angew. Chem. Int. Ed. 47 (2008) 7461–7465.
[10] Y.-K. Sun, S.-T. Myung, H.-S. Shin, Y.C. Bae, C.S. Yoon, J. Phys. Chem. B 110 (2006) 6810–6815.
[11] D. Deng, J.Y. Lee, Angew. Chem. Int. Ed. 121 (2009) 1688–1691, Angew. Chem. Int. Ed. 48 (2009) 1660–1663.
[12] Y.H. Huang, J.B. Goodenough, Chem. Mater. 20 (2008) 7237–7241.
[13] J.M. Paulsen, J.-S. Jeong, K.-Y. Lee, Elecrochem. Solid-State Lett. 10 (2007) A101–A105.
[14] B.J. Hwang, R. Santhanam, C.P. Huang, Y.W. Tsai, J.F. Lee, J. Electrochem. Soc. 149 (2002) A694–A698.
[15] L. Dahéron, R. Dedryvère, H. Martinez, M. Ménétrier, C. Denage, C. Delmas, D. Gonbeau, Chem. Mater. 20 (2008) 583–590.
[16] G.G. Amatucci, J.M. Tarascon, L.C. Klein, Solid State Ioncis 83 (1996) 167–173.
[17] M. Zou, M. Yoshio, S. Gopukumar, J. Yamaki, Chem. Mater. 15 (2003) 4699–4702.
[18] M. Zou, M. Yoshio, S. Gopukumar, J. Yamaki, Chem. Mater. 17 (2005) 1284–1286.
[19] M. Zou, M. Yoshio, S. Gopukumar, J. Yamaki, Elecrochem. Solid-State Lett. 7 (2004) A176–A179.
[20] S. Gopukumar, Y. Jeong, K.B. Kim, Solid State Ioncis 159 (2003) 223–232.
[21] S.-T. Myung, N. Kumagai, S. Komaba, H.-T. Chung, Solid State Ioncis 139 (2001) 47–56.
[22] M. Mladenov, R. Stoyanova, E. Zhecheva, S. Vassilev, Electrochem. Commun. 3 (2001) 410–416.
[23] R. Sathiyamoorthi, R. Chandrasekaran, A. Gopalan, T. Vasudevan, Mater. Res. Bull. 43 (2008) 1401–1411.